Progress In Electromagnetics Research B, Vol. 50, 201–217, 2013

DESIGN OF WLAN BAND NOTCHED UWB MONOPOLE ANTENNA WITH STEPPED GEOMETRY USING MODIFIED EBG STRUCTURE

Gaurav K. Pandey*, Hari S. Singh, Pradutt K. Bharti, and Manoj K. Meshram

Department of Electronics Engineering, IIT (BHU), Varanasi 221005, India

Abstract—A WLAN band notched compact ultra-wideband (UWB) microstrip monopole antenna with stepped geometry is proposed. A L-slot loaded modified mushroom type Electromagnetic Band Gap (EBG) is designed, analyzed and used to realize notched band characteristics for wireless local area network (WLAN) in the UWB frequency range. The proposed antenna having partial ground plane is fabricated on a low cost FR4 substrate having dimensions $40\,(L_{sub}) \times 30\,(W_{sub}) \times 1.6\,(h)\,\text{mm}^3$ and is fed by a 50-Ω microstrip line. The results show that the proposed antenna achieves impedance bandwidth (VSWR < 2) from 2.3 GHz to 11.4 GHz with band notched characteristics (VSWR > 2) from 4.9 GHz to 6 GHz. Fidelity factor for proposed antenna is also analyzed to characterize time domain behavior. Simulation and measurement results of VSWR are found in good agreement.

1. INTRODUCTION

Ultra-wideband technology have become more attractive in academic research and industries for it's vast application in wireless world since the Federal Communication Commission (FCC) released the unlicensed 10-dB band of 7.5 GHz (3.1–10.6 GHz) with an effective isotropic radiated power (EIRP) spectral density of -41.5 dBm/MHz as UWB in year 2002 [1]. UWB systems have advantage of low power consumption, low cost, capability of high data rate, low interference, and ease of installation which is essential for short

Received 1 March 2013, Accepted 1 April 2013, Scheduled 8 April 2013

* Corresponding author: Gaurav Kumar Pandey (gkpandey.rs.ece@itbhu.ac.in).

range communication. Therefore there is increasing demand of UWB antenna which is an integrated component of UWB systems. In addition to UWB, Bluetooth applications have also the advantage of license-free operation in the Industrial, Scientific, and Medical (ISM) band covering frequency range from 2.40 GHz–2.484 GHz (IEEE 802.11b and IEEE 802.11g) band. Bluetooth is also used in short range to transfer data between portable devices with high data rate.

Some standard narrow bands like wireless local area network (WLAN) applications operating in 5.15 GHz–5.825 GHz (IEEE 802.11a and HIPERLAN/2) exists in between the UWB frequency range allocated by FCC which may cause interference to the UWB systems. Therefore, to prevent UWB systems from any interference due to standard narrow bands, band rejection techniques have been used in UWB antenna. In recent years, many type of printed microstrip monopole antenna [2–7] and lots of conventional techniques to achieve the WLAN band notched characteristics have been reported [8–14]. The conventional techniques to achieve band notched are to cut slots on radiating patch, feed line, and on the ground plane or to put some parasitic element near the radiator. But many of them affect the time domain behavior and radiation pattern due to perturbation of radiating element.

Electromagnetic band gap (EBG) structures have been used with microstrip antennas in many applications to reduce surface wave, mutual coupling between to two adjacent antennas [15, 17], use of high impedance screen to provide dipole antenna impedance matching without influence the radiation pattern [16] and to reduce spurious response of filters [15]. EBG structures can also be used in UWB antenna technology to create notched band characteristics [18–21]. In this article, two L-slot loaded modified EBG structure is used to create WLAN band notched in UWB antenna.

The article starts with the design of a compact monopole antenna with stepped geometry. The antenna radiate over the frequency band of 2.3 GHz to over 11 GHz with (VSWR $<$ 2) to cover both ISM band and FCC's UWB. A modified L-slot loaded mushroom type EBG structure is designed and analyzed for determination of operating stop band gap. After that the designed EBG structure is used in the monopole antenna with stepped geometry for WLAN band rejection. The proposed antenna has been designed and optimized by using Ansoft's (HFSS) [22] and also verified by Computer Simulation Technology Microwave studio (CST MWS) [23] before going to final fabrication and measurement steps. Parametric investigations of EBG structure have also been carried out to understand the effects of parameter variation.

2. ANTENNA DESIGN

2.1. UWB Monopole Antenna with Stepped Geometry (Antenna 1)

The configuration of proposed antenna is shown in Figure 1. The antenna consist of partial ground plane, fabricated on FR4 substrate of overall size $40\,(L_{sub}) \times 30\,(W_{sub}) \times 1.6\,(h)\,\text{mm}^3$ with dielectric constant (ε_r) 4.4 with loss tangent $(\tan\delta)$ of 0.02. The radiating element of antenna is composed of three step like sections of size $L_1 \times W_1$, $L_2 \times W_2$, and $L_3 \times W_3$. The size of these sections are determined by using formula for simple patch antenna design [24] for frequencies of 3.5 GHz, 7 GHz, and 10.0 GHz, after that the parameters are optimized to get the UWB characteristics. A 50-Ω microstrip line of width 3 mm with linear tapered transition from 3 mm to 1.2 mm is designed to feed monopole antenna with SMA (sub-Miniature version A) connector. The tapered section in the microstrip line is used to match the impedance over wider frequency band. The optimized shape parameter of the proposed antenna are given in Table 1.

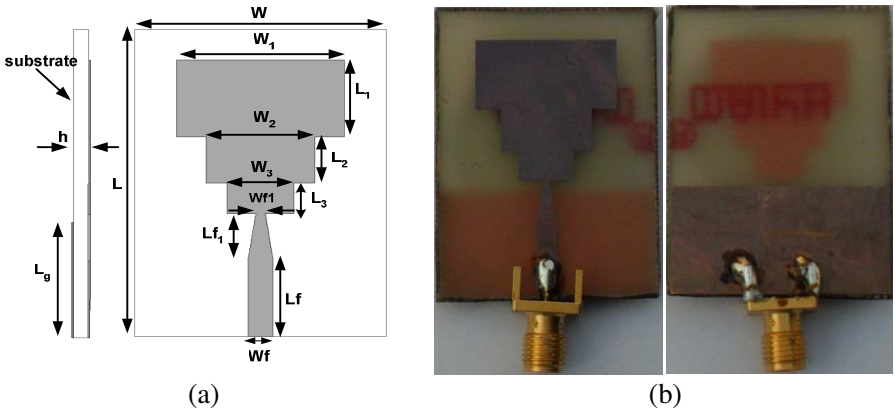

Figure 1. UWB monopole antenna with stepped geometry (antenna 1), (a) HFSS design and (b) Fabricated.

2.2. Design and Study of Modified Mushroom Type EBG Structure

The modified mushroom type EBG consist of square patch with two complementary L-slots loaded and a circular metallic via to connect the patch to ground plane. The stop band of mushroom type EBG

Table 1. Design parameters of UWB Monopole antenna with stepped geometry.

Parameter	Dimension	Parameter	Dimension
L	40 mm	Wf	3 mm
W	30 mm	Wf_1	1.2 mm
h	1.6 mm	Lf_1	6 mm
Lg	15 mm	W_1	20 mm
g	1 mm	L_1	10 mm
Parameter	**Dimension**		
W_2	13 mm		
L_2	6 mm		
W_3	8 mm		
L_3	4 mm		
Lf	10 mm		

depends on the size of patch 'Le_1', radius of via 'r', dimension of slots on patch, height of substrate, and dielectric constant of material. The designed and optimized unit cell of EBG structure is shown in Figure 2 and the optimized value of the shape parameters of modified mushroom type EBG are given in Table 2.

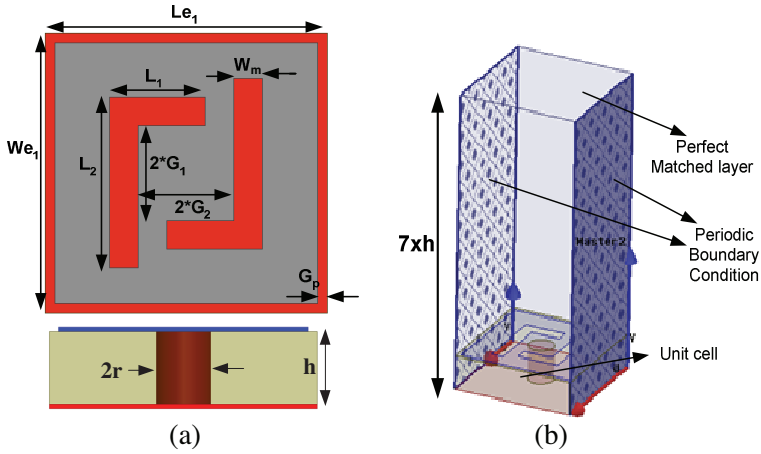

Figure 2. (a) Unit cell of L-slot loaded modified mushroom type EBG and (b) HFSS model to plot dispersion diagram.

Table 2. Parameters of unit cell of EBG structure.

Parameter	**Dimension**	**Parameter**	**Dimension**
Le_1	5.5 mm	G_1	1 mm
We_1	5.5 mm	G_2	1.6 mm
G_p	0.2 mm	r	0.6 mm
h	1.6 mm		
Parameter	**Dimension**		
L_1	2 mm		
L_2	3.6 mm		
W_m	0.6 mm		

The band gap of EBG structure is determined by plotting the dispersion Brillouin diagram shown in Figure 3 using HFSS [22]. The band gap region is defined as a frequency band where no mode is propagated. The band gap from dispersion diagram is seen from 5.12 GHz to 5.98 GHz. Further, the stop band can also be predicted by the plot of variation of S_{21} with frequency by the use of a microstrip line with EBG structure which is shown in Figure 4. It is observed that the $S_{21} < -10$ dB ranging from 4.68 GHz to 6.18 GHz which indicate the stop band behavior of the structure and also in good agreement with the dispersion diagram.

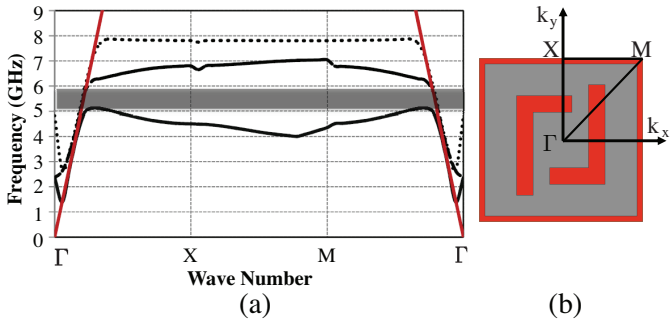

Figure 3. (a) Dispersion Brillouin diagram of modified mushroom type EBG structure obtained by HFSS with periodic boundary conditions (PBC), and (b) representation of reciprocal space with physical space.

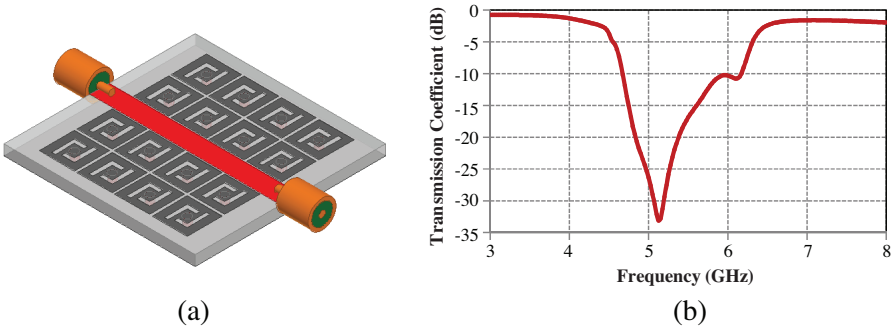

Figure 4. (a) Setup to determine the band gap using Transmission coefficient (S_{21}) and (b) S_{21} variation with Frequency.

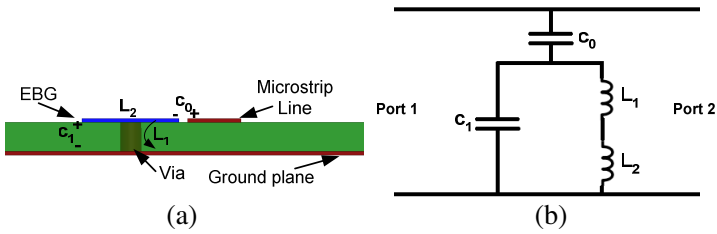

Figure 5. (a) EBG structure in vicinity of microstrip line and, (b) equivalent resonant circuit of (a).

A microstrip line based approach given in [17, 20] is applied to study the resonant frequency characteristics of EBG which is the approach applied to design UWB band notched antennas. As shown in the Figure 5, the complementary L-slot loaded EBG patch is located in vicinity of 50-Ω microstrip line with gap 'G_p'. An equivalent circuit model is designed based on LC resonator to explain the mechanism of the EBG structure coupled to the microstrip feed line. In this model, C_0 denote the capacitance between the EBG patch and microstrip line and C_1 is capacitance between EBG patch and ground plane. The inductance L_1 is due to current flow through the via and L_2 is due to current flow around the L-slots. Then based on the LC-parameters the resonant frequency is given by,

$$f_r = \frac{1}{2\pi\sqrt{(L_1 + L_2)(C_1 + C_0)}} \tag{1}$$

2.3. WLAN Band Notched UWB Monopole Antenna Design (Antenna 2)

To create band notched characteristics for WLAN (IEEE 802.11a) in FCC's UWB frequency range modified slot loaded mushroom type EBG which has it's stop band in the range of WLAN frequency band is used. The Modified mushroom type EBG structure is placed at a distance '$cx = 1$ mm' from bottom of the antenna and on both sides of microstrip feed line of monopole antenna with stepped geometry with gap of 'G_p' to create the desired 5.15 GHz–5.825 GHz WLAN band notched characteristics. The proposed monopole antenna is shown in the Figure 6. The gap 'G_p' is same as the distance of patch sides from substrate corner in unit cell.

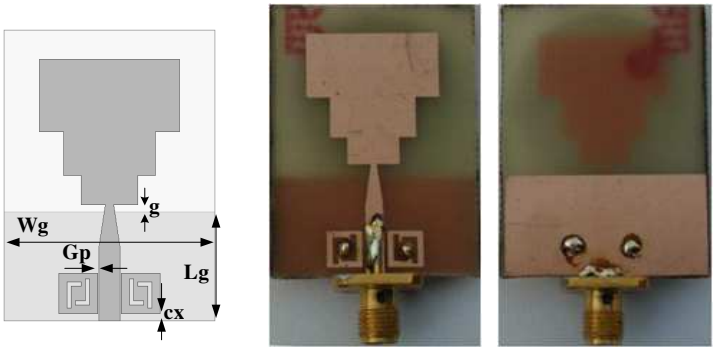

Figure 6. WLAN band notched UWB Monopole antenna with stepped geometry using EBG structure (antenna 2), (a) HFSS Design and (b) fabricated.

3. PARAMETRIC STUDY OF PROPOSED ANTENNA WITH EBG STRUCTURE

To understand the effect of some important parameters of EBG structure on the UWB antenna with stepped geometry simulated parametric study has been done in this section.

The variation of VSWR for different EBG patch size (Le_1) is shown in Figure 7(a). It is clear from figure that Le_1 offer sufficient freedom of selecting the notched frequency. When Le_1 decreases the center frequency of notched band increases with constant bandwidth. Figure 7(b) presents the variation of VSWR with coupling gap (G_p) between EBG patch and feed line. It is observed that with increase

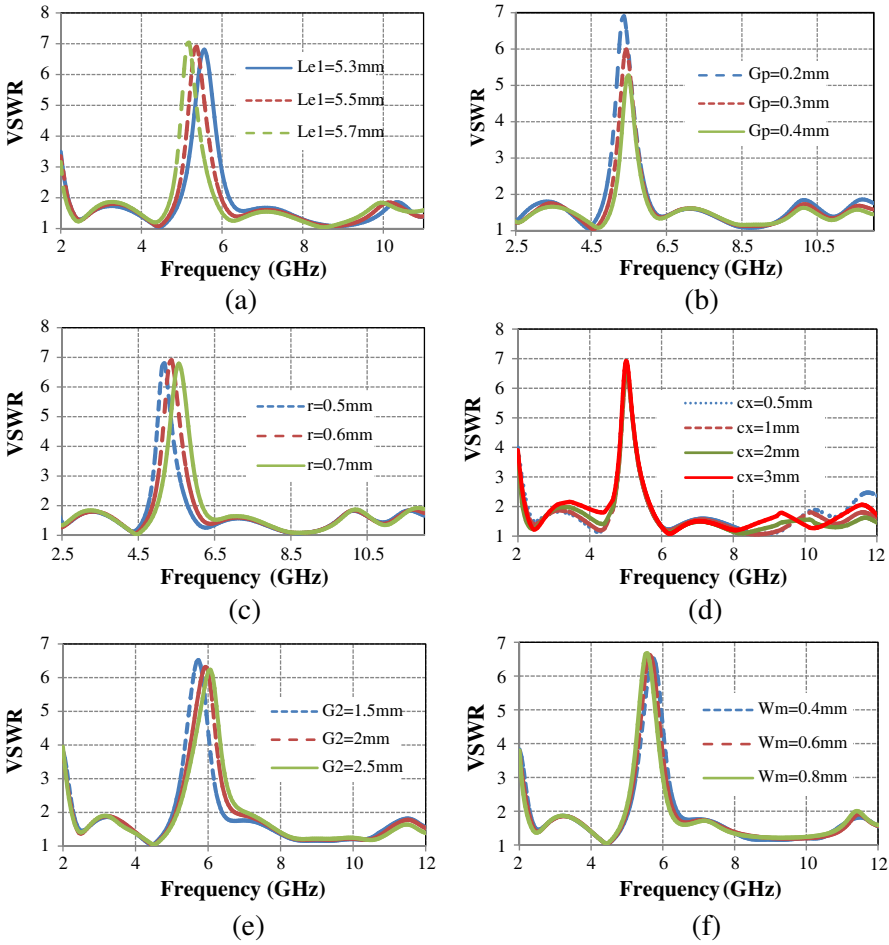

Figure 7. Variation of VSWR with the variation of (a) length of EBG patch Le_1, (b) gap between feed line and EBG patch G_p, (c) radius of via r, (d) position of EBG along feed line cx, (e) distance between L-slots on EBG in vertical direction G_2, and (f) width of L-slot on EBG patch W_m.

of 'G_p', peak value of VSWR decreases and the bandwidth at notched band increases while upper frequency of notched band kept constant. This is due to the reduction of capacitive coupling between EBG and feedline. The radius (r) of via of EBG structure is also an important parameter which include an inductance parameter in equivalent circuit of Figure 5. The effect of variation of 'r' on VSWR plot is shown in

Figure 7(c). It is clear that as the radius of the via decreases, the center frequency of notched band also shifted to lower frequency range with some decrease in bandwidth, it is due to the fact that when the radius of via decreases the inductance related to via increases.

Figure 7(e) presents the effect of variation of distance (G_2) between two L-shaped slots of EBG patch on VSWR pattern. Due to variation of distance the current path on EBG patch increases which add the more inductance value, due to which the bandwidth and center frequency of notched band increases. The variation of VSWR for different width (W_m) of L-slots on EBG patch is shown in Figure 7(f). It is seen that the upper notched frequency decreases with the increase of slot width, which can be used to tune the band precisely.

Further, investigations of the number of unit cell of the proposed EBG structure is carried out on the performance of the antenna. Four different cases are considered as shown in Figure 8. Figure 9(a) shows the variation of VSWR as a function of frequency with the variation of number of elements of EBG structure. In case 1, the value of VSWR and bandwidth of band notched decreases in comparison to case 2 (proposed Antenna 2). This is due to the reduction of capacitive coupling between feed line and EBG structure. When we consider case 3 and case 4, dual band notched characteristics is observed. Therefore, wide notched band is achieved. In case 3, since more unit cells of EBG is directly coupled to feed line, therefore the peak of VSWR value is more than the case 4. However, we have considered the case 2 as optimized structure.

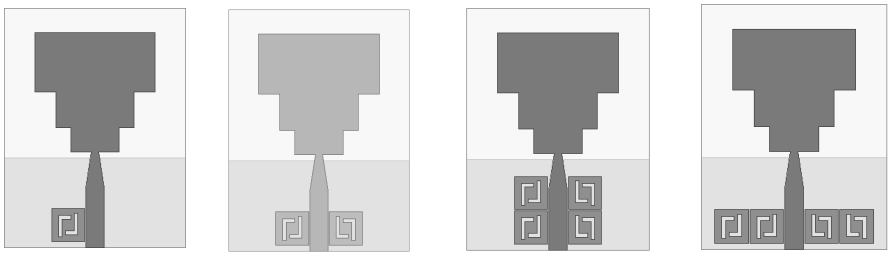

Figure 8. Different cases for the variation of number of unit cell of EBG structure.

Figure 9(b) shows the variation of gap 'g' between ground plane and radiating patch of antenna 2, it is working as a matching network. The optimized value of 'g' is 1 mm since at this value the capacitance between radiating patch and ground plane balances the inductance of antenna. While when we decrease or increase the gap, impedance

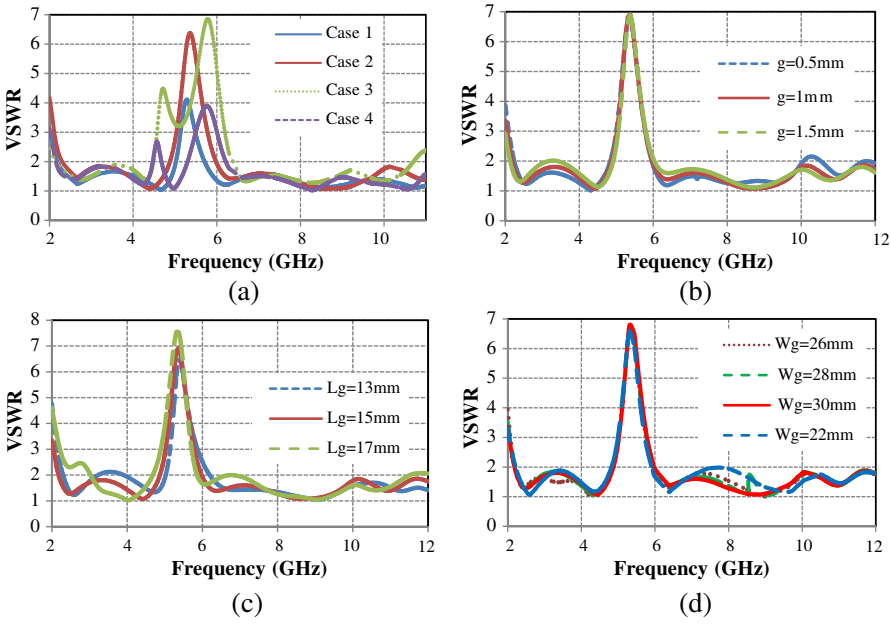

Figure 9. Variation of VSWR with the variation of (a) number of EBG elements in different cases, (b) gap (g) between ground plane and radiating patch, (c) length of ground plane (L_g), and (d) width of ground plane (W_g).

bandwidth at higher and lower frequency deteriorate. The variation of VSWR with variation of length L_g of ground plane is shown in Figure 9(c). It is observed that the optimized value of L_g is 15 mm while when we increase or decrease the length, impedance bandwidth reduces from lower frequency side. From, Figure 9(d) it is clear that the variation of ground plane width 'W_g' also affect the impedance bandwidth but for small variation it is not significant and at value of $W_g = 22$ mm it approaches the VSWR value of 2 in UWB range.

4. MEASURED AND SIMULATED RESULTS

The proposed monopole antenna with stepped geometry has been designed and optimized by Ansoft's HFSS and simulation is also verified by CST MWS. CST MWS is further used for calculation of the time domain behavior of the UWB antenna. The measurement of proposed antenna is done using Agilent E8364B PNA. Figure 10 shows the simulation and measured VSWR variation with frequency of the

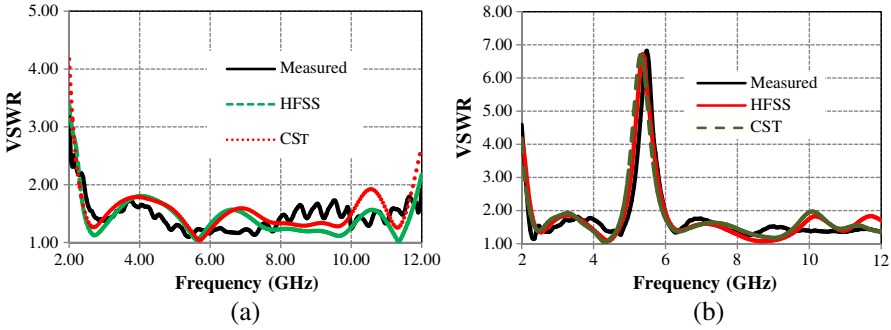

Figure 10. Variation of VSWR with frequency, (a) antenna 1 and (b) proposed antenna 2.

proposed antenna with and without EBG structure. From the plot it is clear that the monopole antenna with stepped geometry shows the impedance bandwidth of 2.3 GHz to over 11 GHz (VSWR < 2). The proposed antenna has sharp band notched from 4.9 GHz to 6 GHz around central frequency of 5.5 GHz with high VSWR. Good agreement between simulation and measurement results is achieved.

To understand the mechanism of antenna, input impedance with variation of frequency is plotted in Figure 11(a). It is seen that the real part and imaginary part of impedance lies around 50-Ω and 0-Ω respectively and oscillate about it throughout the UWB range except for the WLAN frequency region where very high mismatch corresponding to real and imaginary part of impedance occur due to which during that frequency range, power will not be accepted to radiate through antenna.

The surface current distribution of the proposed antenna with EBG structure is shown in Figure 11(b). From figure it is clear that at the frequency of 4 GHz and 8 GHz the maximum current is concentrated and propagated to radiating element while at frequency of 5.5 GHz maximum current is concentrated on EBG structure due to which less current is propagated to antenna to radiate. which confirms the mechanism of EBG structure and the proposed antenna.

Figure 12 presents the comparison of the measured radiation patterns between antenna 1 and antenna 2 at 3 GHz, 4.5 GHz, 7 GHz, and 10 GHz. The radiation patterns of antenna 1 are nearly identical with antenna 2 radiation patterns. Thus, the introduction of EBG structure has little effect on the radiation patterns. It is clear from figure that the antenna have good omnidirectional radiation patterns at 3.0 GHz, however the radiation pattern at higher frequencies such

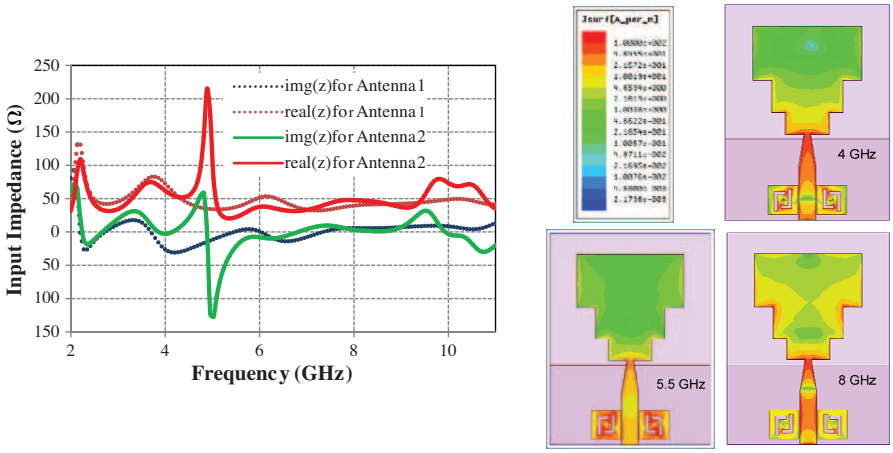

Figure 11. (a) Variation of input impedance of Antenna 1 and Antenna 2, (b) Variation of surface current of antenna 2 at different frequency.

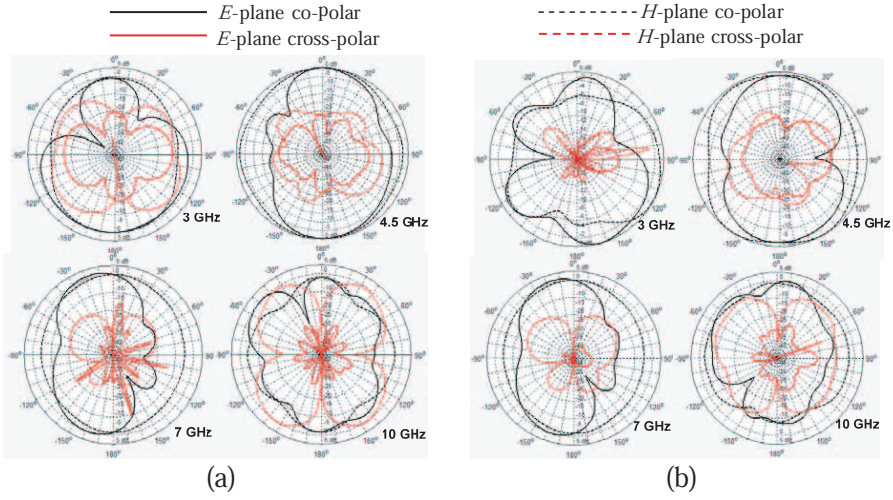

Figure 12. Measured radiation pattern at different frequency, (a) antenna 1 and (b) antenna 2.

as at 7 GHz and 10 GHz shows some variation from omnidirectional properties. However, generally the radiation patterns in E-plane are roughly dumbbell shape and the pattern in H-plane is quite omnidirectional.

The measured gain of the both antenna 1 and antenna 2 is shown in Figure 13(a). It is observed from the plot that the gain drastically decreases and goes to negative in the range of WLAN notched band for Antenna 2 compared to the gain of Antenna 1. A gain suppression of 6 dB is achieved. Otherwise the gain of both the antenna is almost constant in all the frequency range and varies between 2 dBi and 6 dBi. Similar nature is also observed from the plot of variation of radiation efficiency with frequency shown in Figure 13(b). The radiation efficiency is determined by using Wheelar Cap method [25]. From the plot it is clear that during notched band the radiation efficiency decreases up to 30% in the case of antenna 2 while other than notched band, proposed antenna shows good radiation efficiency.

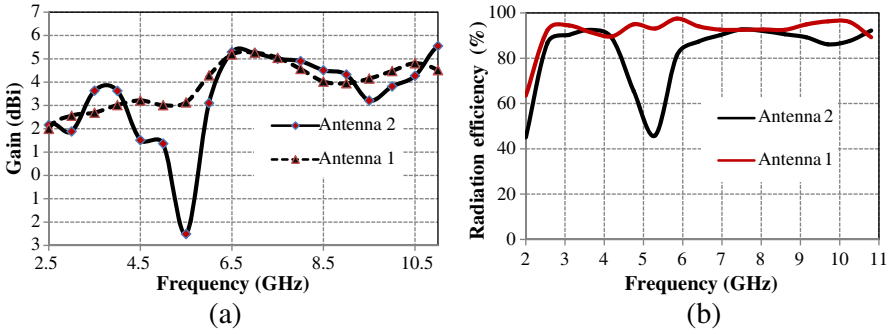

Figure 13. (a) Measured gain of proposed antennas and (b) radiation efficiency of proposed antennas.

The time domain behavior is one of the important characteristics of UWB antennas. The antennas should have minimum distortion in both transmitting and receiving modes. To investigate the time-domain behavior a setup is created in CST MWS. The antennas are placed in two orientation one is face to face and other is side by side with a distance between two antennas is 30 cm (far field position). The transmitting antenna is excited with Gaussian pulse and the signal is received at second antenna to investigate. The normalized signal values of excited and transmitted signal in both the cases are shown in Figure 14. From this it is clear that in both the cases the transmitted signal does not distort significantly than excited pulse.

A well defined parameter fidelity factor [20] which is used to measure the degree of similarity between the input and the received signal, which is defined as

$$F = \max = \left[\frac{\int_{-\infty}^{\infty} s_t(t+\tau)d\tau}{\int_{-\infty}^{\infty} |s_t(t)|^2 dt \int_{-\infty}^{\infty} |s_r(t)|^2 dt} \right] \tag{2}$$

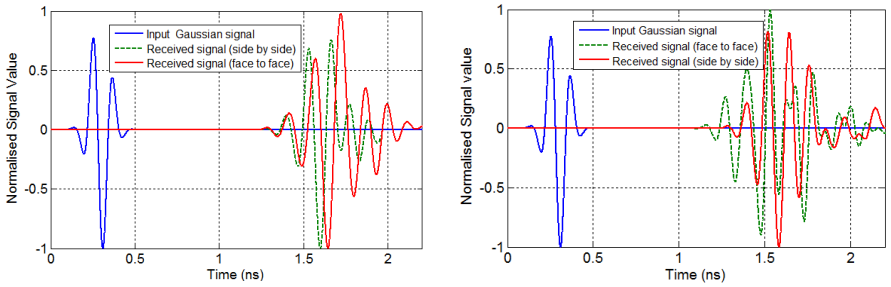

Figure 14. Excited Gaussian pulse and the received pulse at different orientations, (a) antenna 1 and (b) antenna 2.

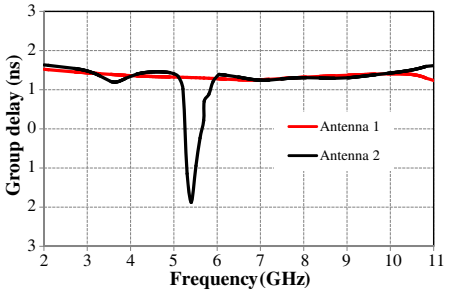

Figure 15. Far field group delay of the proposed antennas.

where, $s_t(t)$ and $s_r(t)$ are input and received signal. The fidelity factor in both the cases with and without EBG is given in Table 3. Then from the time domain results given in Table 3 it is clear that due to the EBG structure signal does not distort in comparison to antenna 1 very much which shows that the time domain behavior of antenna 2 remain approximately same. Table 3 also shows the good pulse handling capability of proposed antenna as required by UWB communication system antennas.

Table 3. Fidelity factor of the proposed antennas.

Orientation	Face to Face	Side by Side
Antenna 1	0.68	0.88
Antenna 2	0.67	0.85

The far field group delay of the proposed antennas is shown in Figure 15. The far field group delay is determined by placing the antenna in side by side position at a distance of 30 cm. It is clear that during notched band the group delay is very high in comparison to other frequencies in UWB range.

5. CONCLUSION

A monopole antenna with stepped geometry for Bluetooth and UWB applications with WLAN band notched to avoid interference in UWB band has been realized and discussed with detailed analysis. The notched band is introduced in the UWB range with the help of two modified L-slot loaded mushroom type EBG placed on the both sides of microstrip feed line. An equivalent resonant circuit model of proposed antenna with modified mushroom type EBG is also given. The stop band of EBG structure is analyzed with the help of dispersion Brillouin diagram and transmission coefficient results. Good agreement is found between simulated and measured results. From the simulation results it can be concluded that the introduction of EBG structure has negligible effect on the radiation patterns and time domain behaviors of the proposed antenna. This antenna can be expected to be a good candidate for UWB applications.

REFERENCES

1. Fedral Communication Commission, "First order and report: Revision of part 15 of the Commision's rules regarding UWB transmission systems," Apr. 22, 2002.
2. Agrawall, N., G. Kumar, and K. Ray, "Wide-band planar monopole antennas," *IEEE Transactions on Antennas and Propagation*, Vol. 46, No. 2, 294–295, Feb. 1998.
3. Clerk, J., J. Liang, C. C. Chiau, X. Chen, and C. G. Parini, "Study of a printed circular disc monopole antenna for UWB systems," *IEEE Transactions on Antennas and Propagation*, Vol. 53, No. 11, 3500–3504, Nov. 2005.
4. Ling, C. W., W. H. Lo, R.-H. Yan, and S. J. Chung, "Planar binomial curved monopole antennas for ultrawideband communication," *IEEE Transactions on Antennas and Propagation*, Vol. 55, No. 9, 2622–2624, Sep. 2007.
5. Kan, Y. C., C. C. Lin, and H. R. Chuang, "A 3–12 GHz UWB planar triangular monopole antenna with ridged ground-plane," *Progress In Electromagnetics Research*, Vol. 83, 307–321, 2008.

6. Xu, H.-Y., H. Zhang, K. Lu, and X.-F. Zeng, "A holly-leaf-shaped monopole antenna with low RCS for UWB application," *Progress In Electromagnetics Research*, Vol. 117, 35–50, 2011.
7. Liang, J., C. C. Chiau, X. Chen, and C. G. Parini, "Printed circular disc monopole antenna for ultra wideband applications," *Electronics Letters*, Vol. 40, No. 20, 1246–1248, 2004.
8. Dong, Y. D., W. Hong, Z. Q. Kuai, C. Yu, Y. Zhang, J. Y. Zhou, and J. X. Chen, "Development of ultra-wideband antenna with multiple band notched characteristics using half mode substrate integrated waveguide cavity technology," *IEEE Transactions on Antennas and Propagation*, Vol. 56, No. 9, 2894–2902, Sep. 2008.
9. Fallahi, R., A. A. Kalteh, and M. Golparvar Roozbahani, "A novel UWB elliptical slot antenna with band-notched characteristics," *Progress In Electromagnetics Research*, Vol. 82, 127–136, 2008.
10. Ryu, K. S. and A. A. Kishk, "UWB antenna with single or dual band-notches for lower WLAN band and upper WLAN band," *IEEE Transactions on Antennas and Propagation*, Vol. 57, No. 12, 3942–3950, Dec. 2009.
11. Yang, Y. B., F. S. Zhang, F. Zhang, L. Zhang, and Y. C. Jiao, "Design of novel wideband monopole antenna with a tunable notched-band for 2.4 GHz WLAN and UWB applications," *Progress In Electromagnetics Research Letters*, Vol. 13, 93–102, 2010.
12. Islam, M. T., R. Azim, and A. T. Mobashsher, "Triple band-notched planar UWB antenna using parasitic strips," *Progress In Electromagnetics Research*, Vol. 129, 161–179, 2012.
13. Chuang, C. T., T. Ju Lin, and S. J. Chung, "A band-notched UWB monopole antenna with high notch-band-edge selectivity," *IEEE Transactions on Antennas and Propagation*, Vol. 60, No. 10, 4492–4499, Dec. 2012.
14. Mishra, S. K., R. Gupta, A. Vaidya, and J. Mukherjee, "Printed fork shaped dual band monopole antenna for bluetooth and UWB applications with 5.5 GHz WLAN band notched characteristics," *Progress In Electromagnetics Research C*, Vol. 22, 195–210, 2011.
15. Yang, F. and Y. Rahmat-Samii, "Microstrip antennas integrated with electromagnetic band-gap (EBG) structures: A low mutual coupling design for array applications," *IEEE Transactions on Antennas and Propagation*, Vol. 51, No. 10, 2936–2946, Oct. 2003.
16. Bianconi, G., F. Costa, S. Genovesi, and A. Monorchio, "Optimal design of dipole antenna backed by finite high-impedance screen," *Progress In Electromagnetics Research C*, Vol. 18, 137–151, 2011.

17. Mäkinen, R., V. Pynttäri, J. Heikkinen, and M. Kivikoski, "Improvement of antenna isolation in hand-held devices using miniaturized electromagnetic bandgap structures," *Microwave and Optical Technology Letters*, Vol. 49, No. 10, 2508–2513, Oct. 2007.
18. Peng, L. and C. L. Ruan, "UWB band-notched monopole antenna design using electromagnetic-bandgap structure," *IEEE Transactions on Microwave Theory and Techniques*, Vol. 59, No. 4, 1074–1081, Apr. 2011.
19. Yazdi, M. and N. Komjani, "Design of a band-notched UWB monopole antenna by means of an EBG structure," *IEEE Antennas and Wireless Propagation Letters*, Vol. 10, 170–173, 2011.
20. Li, T., H. Q. Zhai, G. H. Li, and C. H. Liang, "Design of compact UWB band-notched antenna by means of electromagnetic-bandgap structures," *Electronic Letters*, Vol. 48, No. 11, May 2012.
21. Xu, F., Z. X. Wang, X. Chen, and X. A. Wang, "Dual band-notched UWB antenna based on spiral electromagnetic-bandgap structure," *Progress In Electromagnetics Research B*, Vol. 39, 393–409, 2012.
22. Ansoft's HFSS, [Online], Available: http://www.ansoft.com.
23. CST MWS, [Online], Available: http://www.cst.com.
24. Balanis, C. A., *Antenna Theory: Analysis and Design*, 3rd Edition, 811–876, Wiley India Edition, 2012.
25. Schantz, H. G., "Radiation efficiency of UWB antennas," *IEEE Conference on Ultra Wideband Systems and Technologies*, May 2002.